The maltose ABC transporter in the 21st century – towards a structural-dynamic perspective on its mode of action

Enrica Bordignon, Mathias Grote, Erwin Schneider

molecular microbiology

The maltose ABC transporter in the 21st century – towards a structural-dynamic perspective on its mode of action

Journal:	*Molecular Microbiology*
Manuscript ID:	MMI-2010-10038.R2
Manuscript Type:	MicroReview
Date Submitted by the Author:	21-Jul-2010
Complete List of Authors:	Bordignon, Enrica; ETH Zurich, Physical Chemistry Grote, Mathias; University of Exeter, : ESRC Research Centre for Genomics in Society Schneider, Erwin; Humboldt University of Berlin, Biology/Microbial Physiology
Key Words:	maltose ABC transporter, mechanism, crystal structures, dynamics, regulation

The maltose ABC transporter in the 21st century – towards a structural-dynamic perspective on its mode of action

Enrica Bordignon[1*], Mathias Grote[2§] and Erwin Schneider[2*]

[1] ETH Zurich, Laboratory of Physical Chemistry, Wolfgang-Pauli-Str. 10. CH-8093 Zurich, Switzerland

[2] Humboldt University of Berlin, Department of Biology, Division of Microbial Physiology, Chausseestr. 117, D-10115 Berlin, Germany

[§] Present address: ESRC Research Centre for Genomics in Society (Egenis), University of Exeter, Byrne House, St. German's Road, Exeter EX4 4PJ, UK

Key words: maltose ABC transporter/mechanism/crystal structures/dynamics/regulation

Running title: Maltose ABC transporter in the 21st century

* Corresponding authors

E-mail: enrica.bordignon@phys.chem.ethz.ch. Tel: +41-44-6337570; Fax: +41-44-6331448

E-mail: erwin.schneider@rz.hu-berlin.de. Tel: +49-30-20938121; Fax: +49-30-20938126

This article is dedicated to Prof. Dr. Winfried Boos (University of Konstanz) in recognition of his contributions to the current knowledge on the maltose system

Summary

The maltose/maltodextrin transport system of *Escherichia coli/Salmonella*, composed of periplasmic maltose binding protein, MalE, the pore-forming subunits MalF and MalG, and a homodimer of the nucleotide-binding subunit, MalK, serves as a model for canonical ATP-binding cassette importers in general. The wealth of knowledge accumulated on the maltose transporter in more than three decades by genetic, molecular genetic and biochemical means was complemented more recently by crystal structures of the isolated MalK dimer and of two conformational states of the full transporter. Here, we summarize insights into the transport mechanism provided by these structures and draw the reader's attention to experimental tools by which the dynamics of the transporter can be studied during substrate translocation. A transport model is presented that integrates currently available biochemical, biophysical, and structural data. We also present the state of knowledge on regulatory functions of the maltose transporter associated with the C-terminal domain of MalK. Finally, we will address the application of coarse-grained modelling to visualize the progression of the conformational changes of an ABC transporter with special emphasis on the maltose system, which can provide a model platform for testing and validating the bioinformatic tools.

Introduction

ATP-binding cassette (ABC) - transporters are ubiquitous membrane proteins that mediate the uptake or export of a large variety of solutes ranging from small ions to polypeptides across biological membranes at the expense of ATP (Holland *et al.*, 2003). They are associated with diverse cellular processes, including some of medical importance. ABC transporters share a modular architecture comprising two transmembrane domains (TMDs) and two nucleotide-binding domains (NBDs). The substrate specificity is accomplished by the TMDs, which

display basically no sequence homologies and feature varying numbers of transmembrane helices among different ABC transporters. On the contrary, the ability to bind and hydrolyze ATP, thus providing the energy stroke for substrate translocation, is a common feature of the NBDs, which share several conserved features in all ABC transporters (reviewed in Dawson *et al.*, 2007). With regard to three-dimensional structure, NBDs can be subdivided in a RecA-like subdomain, containing the conserved Walker A and B sites which contribute substantially to nucleotide binding, and a helical subdomain encompassing additional conserved motifs. Among these are the Q-loop (containing a conserved glutamine residue) and the signature sequence ('LSGGQ motif') by which members of the family can be identified. The Q-loop, located at the interface to the TMDs, is known to sense the γ–phosphate, bind the Mg^{2+} ion and attack water, while the signature sequence ('LSGGQ motif') is involved in complexing ATP (reviewed in Oswald *et al.*, 2006).

TMDs and NBDs can be arranged in any possible combination: either as separately encoded protein subunits like in most prokaryotic systems, as half transporters consisting of two copies of a TMD-NBD fusion protein or as a single polypeptide chain. Canonical ABC import systems, hitherto confined to prokaryotes, require an additional component. This add-on has been identified as an extracytoplasmic solute binding protein (SBP) or receptor for substrate capture and initiation of the transport cycle (Davidson *et al.*, 2008; Eitinger *et al.*, 2010). According to Locher (2009), canonical ABC importers can be subdivided into types I and II. The first type comprises smaller importers, such as the maltose or the molybdate/tungstate importers, featuring a transmembrane core of 10-14 helices. Type II importers on the other hand display larger transmembrane domains with up to 20 helices and specificity for metal chelates, heme, and vitamin B_{12}.

For both type I and II importers, the SBPs generally consist of two symmetrical domains joined by a hinge region that flanks the central substrate-binding pocket (Quiocho and Ledvina, 1996). SBPs were most recently re-classified into six clusters based on their three-dimensional structures (Berntsson *et al.*, 2010).

Notably, in prokaryotes a third type of ABC import systems exists, known as ECF (energy coupling factors) transporters, which could be tentatively classified as type III importers. These systems are composed of shared or dedicated energy-coupling modules comprising one conserved TMD (T-component) and two NBDs which require an additional small integral membrane protein (S-component) of yet unknown structure to capture specific substrates (mostly vitamins) (Rodionov *et al.*, 2006; 2009; Eitinger *et al.*, 2010).

This review focuses on the maltose ABC importer (type I) of *Escherichia coli/Salmonella enterica* subspecies *enterica* serovar Typhimurium, encoded within the maltose regulon, which enables the bacteria to feed on maltose and maltodextrins (α-1,4-linked oligosaccharides up to seven glucose units) formed by enzymatic cleavage of starch or glycogen (Boos and Shuman, 1998). The maltose importer ($MalFGK_2$-E) consists of the periplasmic solute binding protein, MalE, the pore-forming hydrophobic subunits MalF and MalG, and a homodimer of the ATPase subunit, MalK[1] (**Fig. 1**). MalE traps the ligand in an inaccessible cleft by moving both domains towards each other, with a twist of ~30° (Spurlino et *al.*, 1991; Sharff *et al.*, 1992; Evenäs *et al.*, 2001; Shilton *et al.*, 1996; Stockner *et al.*, 2005). Liganded MalE has a dual role: it initiates substrate translocation through the inner

[1] Passage of maltose (at µmolar concentrations) and maltodextrins across the outer membrane requires a genetically linked specific maltoporin, a trimeric ß-barrel protein, which is not subject of this article. See Ranquin and van Gelder (2004) for review.

membrane by binding to $MalFGK_2$ and it also communicates the presence of maltose to the chemoreceptor Tar, thereby initiating attractant chemotaxis (Zhang *et al.*, 1999).

The transmembrane subunits MalG and MalF span the membrane six and eight times, respectively. The third and fourth helices of MalF are connected by a long periplasmic loop (MalF-P2) (~ 20 kDa) which is species-specific and apparently confined to MalF homologs of enteric bacteria (Ehrmann *et al.*, 1998).

Based on the primary structure of MalK, the transporter classification system (TC) (http://www.tcdb.org) places the maltose transporter in the CUT1 family, the members of which share a C-terminal extension of their NBDs. In the case of the enterobacterial maltose transporter, the C-terminal domain of MalK has a dual regulatory function: it controls the activity of MalT, the positive transcriptional regulator of the maltose regulon (Boos and Böhm, 2000), and it is the primary site at which dephosphorylated enzyme IIA^{Glc} of the phosphoenolpyruvate phosphotransferase system binds, preventing maltose uptake. This process is known as 'inducer exclusion' within the context of global carbon regulation (Deutscher *et al.*, 2006).

The wealth of knowledge accumulated on the maltose transporter by genetic, molecular genetic and biochemical means (reviewed in Boos and Shuman, 1998; Ehrmann *et al.*, 1998) was complemented in recent years by crystal structures of four conformers of the isolated MalK dimer (Chen *et al.*, 2003; Lu *et al.*, 2005), and of two conformational states of the full transporter (Oldham *et al.*, 2007; Khare *et al.*, 2009). All these structural data contributed substantially to the current view on the transport mechanism of type I ABC importers. Moreover, they set the stage for the application of biochemical and biophysical tools which, together with computational modelling, will eventually lead to an 'in-depth' understanding of

how the transporter works at the molecular level, including its role in the aforementioned regulatory processes.

This article has two aims: (i) to summarize recent achievements, and (ii) to draw the reader's attention to experimental tools which allow the study of the transporter's dynamics during substrate translocation, *i.e.* what happens in between the snapshots provided by the X-ray structures. We also present a model that integrates currently available biochemical, biophysical, and structural data on the maltose transporter and discuss their relevance for physiological functions within the carbohydrate metabolism of the cell.

Crystal structures of the isolated MalK dimer contributed to the understanding of the catalytic cycle of NBDs

The MalK dimer provides the energy for maltose transport by hydrolyzing ATP. Crystal structures of *E. coli* MalK have been solved in two apo (nucleotide-free)-states, one ADP-bound and one ATP-bound state, representing two open, a semi-open and a closed conformation of the dimer, respectively (Chen *et al.*, 2003; Lu *et al.*, 2005). These structures extended the knowledge on the catalytic cycle of NBD dimers based on various crystal structures of soluble NBDs and biochemical evidence (reviewed in Oswald *et al.*, 2006; Jones *et al.*, 2009).

A stable MalK dimer interface is formed in all states by the C-terminal regulatory domains which are lacking in most other NBDs studied (**Fig. 2**). In contrast, the appurtenant NBDs, consisting each of a RecA-like and a helical subdomain, are subject to large rigid body motions relative to each other in the transition between the different states (**Fig. 2**). Closure and reopening of the MalK dimer has been described as ‘tweezers-like’, with the C-terminal

domain representing the 'handle' and the N-terminal domains being the 'tips' of the tweezers (Chen *et al.*, 2003). Distance changes during the catalytic cycle of $MalK_2$ are particularly large between the Q-loop regions that connect RecA-like and helical subdomains. However, the MalK dimer does not undergo a simple planar movement. Dimer closure is accompanied by an intra-monomer rotation of the helical subdomains towards the RecA-like subdomains, enabling the LSGGQ-motif to contact ATP across the dimer interface.

Interactions of an ATP molecule with the Walker A site of one monomer and the LSGGQ motif of the opposing monomer was previously observed in the structure of the Rad50 protein (an ABC protein not involved in transport) (Hopfner *et al.,* 2000) and was suggested for $MalK_2$ by vanadate-induced photocleavage (Fetsch and Davidson, 2002). In contrast, the dimer structure of the MalK homolog from the hyperthermophilic archaeon *Thermococcus litoralis* (Diederichs *et al.*, 2000) solved earlier showed the NBDs in a different orientation which most likely represents a crystal artifact (discussed in Oswald *et al.*, 2006).

The 'tweezers-like' motion of $MalK_2$ was subsequently also corroborated by molecular dynamics (MD) simulations. Oloo *et al.* (2006) induced a transition from the open to the semi-open and from the semi-open to the closed conformer of $MalK_2$ upon docking of Mg-ATP to the binding pockets (see **Fig. 2**). The simulation highlighted that completion of closure was driven mainly by cross-interface contacts between residues of the LSGGQ-motif and the γ-phosphate of the ATP molecule bound to the opposing monomer. Wen and Tajkhorshid (2008) found that hydrolysis of one ATP was sufficient to trigger dimer opening *in silico* and that separation of the LSGGQ-motif from the nucleotide was the key step of this process.

The catalytic cycle of the NBDs in the full transporter: effects of TMDs and MalE

In recent years, it has been thoroughly investigated how the catalytic cycle of the NBDs in the full transporter is affected by the interacting TMDs and by the substrate availability communicated via MalE.

The maltose transporter solubilised in detergent micelles was found to hydrolyse ATP independently of the presence of liganded MalE (Davidson *et al.*, 1992; Landmesser *et al.*, 2002). Similarly, the isolated $MalK_2$ domains are also known to exhibit a spontaneous but low ATPase activity (Morbach *et al.*, 1993). In the case of the full transporter, however, ATPase activity is substantially increased by adding liganded MalE (Davidson *et al.*, 1992; Landmesser *et al.*, 2002), showing tighter coupling in the complete system.

The problem of ATP-induced MalK-dimer closure and coupling to substrate transport was also addressed by spin-labeling electron paramagnetic resonance (EPR) spectroscopy and cross-linking performed with purified transport complexes in detergent micelles. In the absence of MalE and maltose, a measurable distance change between Q-loop residues of the full transporter's MalK subunits was observed. This distance change, however, became much less pronounced when the transporter was reconstituted in a lipid environment (Daus *et al.*, 2007b; Grote *et al.*, 2008; 2009). The observed ATP-induced (partial) closure of the MalK dimer in detergent solution in the absence of MalE is perfectly in line with the proposed futile ATP hydrolysis cycle observed under these conditions. The fact that this effect was not found in the membrane-reconstituted system could be explained by an impact of membrane lateral pressure on the coupling between TMDs and NBDs. It is tempting to speculate that ATP is spontaneously hydrolyzed in micelles due to a lower energy barrier between the open and closed $MalK_2$ conformations, which statistically enhances closing events in the absence of substrate.

EPR analyses demonstrated a profound effect of liganded MalE on the closure of the NBDs. In fact, the (partial) closure solely induced by ATP binding (Grote *et al.*, 2008) could be turned to 'full' closure in the presence of substrate-loaded MalE both in micelles and in proteoliposomes (Grote *et al.*, 2009; Orelle *et al.,* 2009) which correlates with the highest ATPase activity observed.

Interestingly, trapping the transporter in a transition state by the inhibitor vanadate after hydrolysis of 1 ATP (Chen *et al.*, 2001) did not reopen the NBDs as monitored by cross-linking (and contrarily to what was predicted by MD simulation in the isolated NBDs, see above) (Daus *et al.,* 2007b; Grote *et al.*, 2008). However, ATP-hydrolysis was shown to induce a semi-open state of the NBDs in intact transporters that resembles the effects observed in the isolated domains, thus corroborating the idea of a tweezers-like motion in the assembled complex as well (Orelle *et al.,* 2008).

Communication between the periplasmic and the cytoplasmic regions of the transporter seems to be strictly mediated by SBP also in other types of ABC importers. For example, the vitamin B_{12} binding protein, BtuF, induces conformational changes in the cytoplasmic gates of the cognate $Btu(CD)_2$ transporter already in the absence of nucleotides (Hvorup *et al.*, 2007), and the response of the cytoplasmic gates during the nucleotide cycle is completely dependent on BtuF (Goetz *et al.*, 2009). One might speculate that the transmembrane S-component of the candidate type III (ECF) importers could be the cognate TMD partner of the energy-coupling modules, thus potentially relevant for the overall conformation of the transporter at all stages of substrate translocation as well.

Crystal structures of the full transporter: insights into the transport mechanism

The maltose transporter is currently the only ABC importer for which two X-ray structural models exist in the apo and ATP-bound states (Oldham *et al.*, 2007; Khare *et al.*, 2009). They represent two snapshots of what is now recognized to be the inward-to-outward transition, coupling ATP hydrolysis to the NBDs' and TMDs' conformational changes. Both structures together with those available for the molybdate/tungstate transporters of *Archaeglobus fulgidus* (Hollenstein *et al.*, 2007) and *Methanosarcina acetivorans* (Gerber *et al.*, 2008), and the methionine transporter of *E. coli* (Kadaba *et al.,* 2008) corroborate the hypothesis of a unifying mechanism of action of type I importers ('alternating access model', see below).[2]

The X-ray structure of the nucleotide-free (apo) state[3] of $MalFGK_2$ is available only at low resolution (4.50 Å) (Khare *et al.*, 2009). The crystal was obtained in the absence of nucleotides and MalE, and the complex was stabilized by removal of helix 1 of MalF (which is known to be dispensable for function; Ehrmann *et al.*, 1998). The complex shows a clear inward facing conformation of the two TMDs (**Fig. 1**). Superposition of the backbone atoms of transmembrane cores of MalF and MalG with the pore-forming subunits ModB of the molybdate/tungstate transporter of *A. fulgidus* and MetI of the methionine transporter of *E. coli* in the inward facing conformations indicate a common overall configuration of the TMDs of type I importers in the apo-state (Khare *et al.*, 2009).

[2] The vitamin B12 type II transporter, for which a distinct mechanism of action was suggested, has also been crystallized in two states (absence and presence of BtuF), one of which might correlate with the resting state. However, no structure with bound nucleotides is currently available (Locher et al., 2002; Hollenstein et al., 2007).

[3] In this review, the term apo-state is preferred to the term "resting state" for the complex in the absence of nucleotides. In fact, the "resting state" of the transporter *in vivo* can be considered to be ATP-bound, due to the high ATP concentrations inside the cell.

The periplasmic regions of the complex are only poorly resolved in the structure. In particular, the MalF-P2 loop is missing, probably due to a high degree of disorder which might be either a crystal packing artifact or an intrinsic property of the loop in the apo state.

The crystal structure of the complex in the presence of ATP and MalE was resolved at 2.8 Å, revealing that MalFG are in a periplasmically open state (**Fig. 1**). The TM helices are in an intertwining configuration, which contrasts the rather parallel arrangement seen in the structures of type II importer $Btu(CD)_2$-F (Hvorup *et al.*, 2007) and the putative metal transporter HI 1470/1 (Pinkett *et al.*, 2006). However, a pseudo-twofold symmetry is observed for the core region of the two proteins, consisting of helices 3-8 in MalF and 1-6 in MalG. These helices can be described as two crescents with their concave sides facing each other. Notably, the first two helices of MalF are positioned away from the dimer interface which is consistent with the earlier finding that helix 1 is dispensable for function (Ehrmann *et al.*, 1998).

The complex used for the crystal contains a Glu-159Q substitution in MalK, which prevents ATP from being hydrolyzed. This results in an ATP-bound structure, which is thought to represent the transition state for ATP hydrolysis. The crystal shows an open (unliganded) MalE bound to the periplasmic side of the complex, a maltose molecule bound solely to a transmembrane region of MalF, and a closed conformation of the ATP-bound $MalK(Glu\text{-}159Q)_2$ subunits. The latter is essentially identical to the closed form of ATP-bound soluble $MalK_2$, with the exception of the Q-loops (Oldham *et al.*, 2007). These are both flexible in the soluble form and well-ordered (β-strand) in the complex structure (Oldham *et al.*, 2007), indicating a stabilization of these NBD regions by the TMDs. This nicely confirmed earlier genetic and biochemical evidence for the interaction between the Q-loops of $MalK_2$ and the so-called 'EAA loops' (subsequently also termed 'coupling helices' or 'L-

loops' based on structural evidence, see below) of MalFG (Mourez *et al.*, 1997; Hunke *et al.*, 2000; Daus *et al.*, 2007b).

Interestingly, the crystal structure of the apo-state shows a β-stranded Q-loop only in the MalK subunit facing MalF, while the Q-loop of the opposing MalK subunit facing MalG is unstructured. Moreover, the C-terminal tail of MalG (residues 290-296), which in the catalytic intermediate is protruding into the dimer interface of MalK, contacting both Q-loops, is completely unresolved in the apo-state. Together with the observed slight asymmetry of the MalK dimer closure based on the X-ray data, this raises the question of whether MalE binding or closure of the MalK dimer stabilizes the Q-loop at the MalK-MalG interface.

The coupling helices of MalF and MalG, which comprise a sequence motif that is conserved among canonical ABC importers and was first recognized for MalG by Dassa and Hofnung (1985), are situated in a cleft on top of each MalK monomer (Oldham *et al.*, 2007). The crystal structure provides insight into various interacting residues in this region, the most important being perhaps a salt bridge between Arg-47 of each MalK monomer and the glutamates of the EAA-motifs (MalF, Glu-401; MalG, Glu-190). Other sites of interaction in the coupling helices are formed by MalF(Met-405) and MalG(Leu-94), both of which pack into a hydrophobic pocket of the respective MalK monomers. Results from mutational analysis (Mourez *et al.*, 1997) and cross-linking (Hunke *et al.*, 2000; Daus *et al.*, 2007b) indicated that both coupling helices might act asymmetrically during the transport cycle. None of the currently available crystal structures provide a clue in favour of this notion.

Substrate is probably translocated through a large solvent-filled cavity that appears to be completely shielded from the membrane and sealed by open MalE in the crystallized state. The substrate-binding site in the crystal involves ten residues of the MalF subunit that contact maltose through H-bonds, van der Waals interactions and aromatic ring stacking. The

crystallized maltose binding site correlates to previous biochemical data showing that substitution of any of six of these residues reduced transporter activity *in vivo* (Ehrle *et al.*, 1996; Steinke *et al.*, 2001). To date, this is the only proof for a distinct substrate-binding site within the transmembrane domains of an ABC importer.

Periplasmic loop regions of MalF and MalG are presumably also involved in functional interactions within the complex. Periplasmic loop P3 of MalG points into the empty ligand binding site of MalE, which led Oldham *et al.* (2007) to propose a 'scoop-like' function for this domain, allowing substrate release from the receptor.

Most prominently, the unusually long second periplasmic loop of MalF (MalF-P2, ~180 amino acids) which folds into an Ig-like domain in the crystal structure and extends some ~30 Å into the periplasm is forming a cap on top of MalE. This position of MalF-P2 might well reflect an intermediate in the catalytic cycle of $MalFGK_2$, but data are not available on its structure or position in the crystal structure of apo-state of the transporter (see above). However, an NMR solution structure of the isolated MalF-P2 polypeptide (encompassing residues Asn-93 to Lys-275) revealed a well-defined tertiary structure similar to that found in the crystal (Jacso *et al.*, 2009). This finding also highlights the ability of this domain to become autonomously folded even in the absence of MalE. Moreover, liganded (closed) MalE was demonstrated to bind to the transporter even in the apo-state (Grote *et al.*, 2009; Daus *et al.*, 2007a; 2009).

The crystal structures also provided some hints on the possible mechanism of a class of maltose transporter mutants functioning independently of the binding protein (Covitz *et al.*, 1994; reviewed in Boos and Shuman, 1998). The mutations which map to transmembrane regions of MalF and MalG are thought to cause the transporter to reside in a transition state-like conformation (Mannering *et al.*, 2001; Daus *et al.*, 2006; 2007b; 2009). All mutations lie

at sites of interaction that are altered in the inward-to-outward transition. The authors speculate that the mutations might lower the energy barrier between the two conformations, facilitating their interconversion in the absence of the binding protein (Khare *et al.*, 2009).

Together, the currently available crystal structures of $MalFGK_2$ clearly confirm the alternating access mechanism of substrate transfer for the type I importers. Conformational changes generated in the NBDs by ATP- and MalE- binding and subsequent ATP hydrolysis cause a shift between a periplasmic-open and a cytoplasmic-open state of the TMDs. The available structures of the molybdate/tungstate transporter, $ModB_2C_2$, of *Methanosarcina acetivorans* (Gerber *et al.*, 2008) and the *E. coli* methionine transporter, $MetI_2N_2$, (Kadaba *et al.,* 2008) (both type I) conform to the proposed inward-facing conformation in the absence of ATP.

Dynamics of the maltose transporter

Although X-ray crystallography has revealed two snapshots of the maltose transporter (apo- and catalytic state), with molecular details on the subtle and concerted interconnection between the different subunits, a complete description of the transport mechanism would require a full understanding of (i) the effects of MalE (unliganded or maltose-loaded) on ATPase activity, (ii) signal transduction from periplasmic loops via TMDs to NBDs, (iii) dynamics of protein regions that communicate, and (iv) the time line of the events. For the first two aspects, some experimental data are already available which will now be discussed.

Interactions with MalE initiate the transport process

In an EPR study of the assembled transporter reconstituted into proteoliposomes, Orelle *et al.* (2008) showed that full closure of ATP-bound $MalK_2$ occurs only upon docking of liganded MalE to the TMDs. However, the conditions of MalE binding to the complex in its different conformers are not yet fully clarified. A stable $MalFGK_2$-E complex is only formed in the vanadate-trapped state or by certain mutations affecting MalK (Chen *et al*., 2001; Oldham *et al.*, 2007).

Liganded MalE was also shown to bind to the apo-state of the transporter (Austermuhle *et al.*, 2004; Daus *et al.*, 2009). Moreover, the relative positions of MalE and the periplasmic regions of MalF (P2-loop) were found by cross-linking to change upon binding of ATP, revealing a motion of MalE correlated with the transporter and its close contact to MalF-P2 in both states (Daus *et al.*, 2009).

The observed binding of unliganded MalE to the transporter was assumed on the basis of its weak stimulatory effect on ATPase activity (Davidson *et al.*, 1992) and corroborated by EPR (Austermuhle *et al.*, 2004). A close contact of unliganded MalE with MalFG was found also in the nucleotide-free state of the complex. Residues Gly-13 and Asp-14 of MalE were identified as sites of interaction with the first periplasmic loop of MalG (Daus *et al.*, 2007a), thereby corroborating genetic analyses (reviewed in Shilton, 2008). Contacts of MalE to the second periplasmic loop of MalF were also detected (Daus *et al.*, 2007a). One way of understanding this finding was provided by a paramagnetic-NMR study that showed that open and closed forms of MalE are in equilibrium even in the absence of substrate (Tang *et al.*, 2009). However, Gould *et al.* (2009) propose that the open, substrate-free conformer of MalE is indeed able to stimulate ATPase activity directly by binding to a still undefined conformer of $MalFGK_2$.

How substrate availability in the periplasmic space is signalled to the cytosolic ABC subunits to induce ATP hydrolysis is still poorly understood. As already discussed, there is experimental evidence for binding of MalE to the apo-state of the transporter regardless of the presence of maltose. The affinity of binding is rather low (upper µM range) but might be compensated for by the 30-to 50-fold molar excess of MalE over the $MalFGK_2$ complex observed *in vivo* (Daus *et al.*, 2007a and references therein).

Recognition of substrate by $MalFGK_2$ could require that N- and C- terminal lobes of MalE bind to the transporter with a different degree of affinity depending on the presence of substrate (suggested by Austermuhle *et al.*, 2004). In agreement with this notion, the ATPase activity of $MalFGK_2$ is coupled to translocation of maltose solely by interactions between $MalFGK_2$ and MalE, independently of the chemical nature of the substrate (Gould and Shilton, 2010). The increase in ATPase activity observed in the presence of unliganded MalE could be reconciled with the previous hypothesis by considering that either the fraction of closed MalE (Tang *et al.*, 2009) stimulates hydrolysis, or a distinct mode of activation exists that involves binding of the open form.

Communicating substrate availability to the NBDs via the unique MalF-P2 loop

As clearly elucidated by the crystal structure of the catalytic intermediate, the large periplasmic MalF-P2 domain plays a major role in MalE recognition and possibly in inter-domain communication. Although apparently confined to MalF homologues from enteric bacteria, earlier genetic studies revealed its functional importance as insertions/deletions were not tolerated with respect to transport (Tapia *et al.*, 1999). In the assembled transporter, MalF-P2 undergoes conformational changes throughout the catalytic cycle as determined by EPR

(Grote *et al.*, 2009). Moreover, rearrangements of MalF-P2 were found to be strictly dependent on ATP and liganded MalE, analogously to what was observed in the MalK dimer closure. Three distinct conformations of MalF-P2 were found, which strikingly correlate with the open, close and semi-open conformation of the NBDs. This result highlights the complex mode of communication between cytoplasmic and periplasmic subunits of the transporter.

The crucial role of the MalF-P2 loop immediately poses the questions of how substrate availability is signalled in the majority of type I importers that lack extended periplasmic loop regions and what is the particular function of the P2 loop in enterobacterial maltose transport systems. Both questions are among those that will have to be addressed in the near future.

Model of maltose transport – paradigm for type I ABC importers?

A dynamic model for the coupling of ATP-hydrolysis and substrate transfer in $MalFGK_2$-E is presented, based on our findings combined with the X-ray and biochemical data discussed above (**Fig. 3**). The transporter is present in an equilibrium of conformers that is modulated by the concentrations of cofactors and interaction partners. Net transport of substrate is achieved by fine-tuning of the transition rates between the different conformational states. The main features of our model are (i) the general alternating access principle, (ii) the persistent interaction of liganded MalE with apo-, ADP- and ATP-bound conformers of $MalFGK_2$, and (iii) the mutual dependency of conformational changes in MalF-P2 and $MalK_2$, leading to a central conformer with closed NBDs and outward-facing TMDs. This intermediate state can presumably be stabilized only by preventing immediate ATP hydrolysis through, e.g. mutations or absence of the Mg^{2+} cofactor. Otherwise, the equilibrium is

strongly shifted towards the ADP-bound conformer with semi-open NBDs and TMDs flipped back towards the cytoplasmic open state, thus releasing maltose into the cytoplasm.

With respect to its details, the model represents the specific situation of the maltose system. However, in the Btu$(CD)_2$-F complex, which might have a distinct mechanism of transport, both BtuF and nucleotides are necessary for the conformational changes in the gates as well (Goetz *et al.*, 2009). An unstable intermediate that depends on the simultaneous presence of two cofactors (receptor/substrate and ATP) seems to be the key determinant step for the mechanism of import for both type I and II importers. In the latter, however, the notion that they might operate on a different scheme is gaining confidence (Goetz *et al.*, 2009; Lewinson *et al.*, 2010). Binding of ATP is suggested to release BtuF, which is opposite of what happens in the maltose system, but reminiscent of what was proposed for the oligopeptide transporter, OppABCDF, of the Gram-positive bacterium *Lactococcus lactis,* (Doeven *et al.*, 2008) (a type I importer!). Nonetheless, an alternating access mechanism could still be the main conformational switch for type I and II importers. However, it might occur in an asymmetric fashion and with the inward- and outward- facing conformations probably at somewhat different timings with respect to the nucleotide cycle. Also with respect to the still unknown mechanism of action of candidate type III importers, there is clearly considerable mechanistic diversity within the large protein super-family of ABC importers.

The regulatory C-terminal domain of MalK

As mentioned in the Introduction, the maltose transporter is involved in regulatory processes via the C-terminal domains of the MalK subunits. Dephosphorylated $EIIA^{Glc}$ blocks maltose transport by inhibiting the MalE/maltose-induced ATPase activity of the transporter, as

demonstrated with purified protein components in proteoliposomes (Landmesser *et al.*, 2002; Samanta *et al.*, 2003). Mutations conferring resistance to $EIIA^{Glc}$ map in two regions in the N- and C-terminal domains of MalK, respectively, which are on the same face of the MalK dimer (Samanta *et al.*, 2003). Two surface-exposed patches were also identified on $EIIA^{Glc}$ that interact with MalK (Blüschke *et al.*, 2006). Moreover, the amphipathic N-terminal domain of $EIIA^{Glc}$, which is thought to function as a membrane anchor (Wang *et al.*, 2000), is crucial for inhibition of the transporter (Blüschke *et al.*, 2006). Cross-linking experiments further revealed that binding site 2 of $EIIA^{Glc}$ (encompassing residues 118 to 127) is close to the C-terminal domain of MalK under all conditions tested, while site 1 (consisting of residues 69-79 and 87-91) is particularly close to residues from the helical subdomain of ADP-bound MalK. Based on these data, a model of the interaction of $EIIA^{Glc}$ with $MalK_2$ was created using the Zdock server at http://zdock.bu.edu/ (**Fig. 4**). Interestingly, docking could only be obtained when using the coordinates of the ADP-bound conformer of isolated $MalK_2$. Thus, we propose that inhibition of the transporter by $EIIA^{Glc}$ is caused by blocking conformational changes subsequent to ATP hydrolysis that are associated with the release of ADP and/or re-binding of MgATP. A molecular dynamics simulation study on the MalK dimer indicated a decrease in size of the putative $EIIA^{Glc}$ binding sites upon nucleotide binding by ~ 4 Å (Oloo *et al.*, 2006). The authors speculated that $EIIA^{Glc}$ might prevent this conformational change, thereby suppressing MgATP binding. Whether one or two copies of $EIIA^{Glc}$ are necessary for blocking the conformational changes of the NBDs is still unknown.

MalT, the positive transcriptional regulator of the maltose regulon and a member of the STAND (signal transduction ATPases with numerous domains) class of P-loop NTPases (Leipe *et al.*, 2004) is a multi-domain protein of 103 kDa. The protein is active in the presence of ATP and maltotriose, which drive its association into homopolymers (Larquet *et al.*, 2004).

While ATP hydrolysis is dispensable for transcription activation, it is required for resetting the inactive (monomeric) state of MalT (Marquenet and Richet, 2007). Maltotriose binding is antagonized by the ATP-bound form of MalK and by two other proteins, MalY and Aes (Joly *et al.*, 2004), which lock MalT in the inactive form. Control of MalT activity by MalK is thought to couple induction of the maltose regulon to internalization of maltodextrins (Boos and Böhm, 2000). Mutations affecting the interaction with MalT cluster near the bottom of the C-terminal domain of MalK but are distinct from those involved in $EIIA^{Glc}$ binding (Samanta *et al.*, 2003). Replacement of Pro-72 in the N-terminal domain of MalK by leucine also caused a regulation-minus phenotype (Böhm *et al.*, 2002). Mutations that render MalT insensitive to inhibition by MalK mostly localize to helices 10 and 11 of domain 3 (DT3) of MalT (Richet *et al.*, 2005), which together with the (ATP-binding) domain 1 (Joly *et al.*, 2004), provides two surface patches for interaction with the MalK dimer. How MalK competes with maltotriose for MalT binding is not yet understood, but it was speculated that MalK prevents maltotriose from gaining access to its binding site within a tunnel formed by domain 3 (Steegborn *et al.*, 2001; Richet *et al.*, 2005; Danot, 2010).

The chemical nature of the MalK-MalT interaction remains to be elucidated. The phenotype of the MalK(Pro-72L) mutation has led to the hypothesis that, as in case of $EIIA^{Glc}$, MalT-DT3 might bind to a surface of the MalK dimer encompassing residues from the N- and C-terminal domains (Richet *et al.*, 2005). This would explain how conformational changes of $MalK_2$ that occur upon ATP binding/hydrolysis are communicated to MalT, since neither the crystal structures (Chen *et al.* 2003) nor a molecular simulation study (Oloo *et al.*, 2006) provided evidence for motional changes of the C-terminal domains during the catalytic cycle. Nevertheless, the data supporting this idea are not convincing. First, the loss in regulation caused by the Pro-72L substitution is substantially smaller than that observed with

most substitutions affecting residues in the C-terminal domain. Moreover, in the crystal structures of the complete transporter, Pro-72 and the proposed C-terminal interaction site are not on a common surface. Thus, further experiments, e.g. co-crystallization of the transporter with the DT3 fragment of MalT, will be required to identify the binding surfaces on both proteins.

Perspectives

Coarse-grained modelling of substrate translocation: the maltose transporter as a model system

Crystal structures of intact transporters provide the molecular basis for understanding the transport cycle. However, they cannot elucidate the dynamics encoded in the protein domains or the exact sequence of events during all steps of the translocation process. Modelling a transporter 'in action' during substrate translocation could be achieved by starting from such crystal structures, and adding the available biochemical and biophysical data on the different states of the translocation process.

By providing distance restraints and a dynamic perspective focused not only on single conformers but on their interconversion, cross-linking, FRET, NMR, and site-directed spin labelling EPR are complementary tools applicable to large functioning protein complexes. Moreover, these can be studied in detergent solution and embedded in liposomes or as recently demonstrated also in nano-discs (Zou and Mchaourab, 2010; Alvarez et al., 2010). Together with coarse-grained modelling tools (for a recent review see Bahar *et al.*, 2010), they open up the possibility to model multiple steps of the transport cycle on the basis of X-ray snapshots or low resolution data.

The maltose system, for which two conformational states have already been trapped by crystallography, provides a unique opportunity for testing and validating modelling approaches to be subsequently applied to the other types of importers and exporters.

Results from dynamic studies such as those mentioned above will surely influence the overall picture of how energy generation and transmembrane transport are coupled in biological macromolecules. Rather than aligning snapshots of crystal structures, the models thus established will depict states of macromolecules as conformational equilibria that are shifted by the respective cofactors (see **Fig. 3**). Moreover, these models will be able to encompass data on flexible regions of the proteins that are underrepresented in crystal structures, but which might play vital roles in the interactions between components.

Evolutionary relationship with ECF (candidate type III) ABC importers?

In 2006, bioinformatic analysis of whole genome sequences from bacteria and archaea led to the recognition of ECF-type importers as an abundant subclass of ABC transporters. (Rodionov *et al.*, 2006). Intriguingly, at least certain substrate-specific (S) components of these transporters can function autonomously as secondary, potentially proton motive force - driven, transport systems in the absence of their cognate NBDs (Hebbeln *et al.*, 2007). The modular architecture of ECF transporters is reminiscent of binding protein-independent maltose transporter mutants (Covitz *et al.*, 1994). Thus, it is tempting to speculate that the MalFG subunits of these mutants might also be able to operate in a secondary transporter mode in the absence of MalK. In this respect, it is noteworthy that a pmf-driven activity was demonstrated for LmrA, a multidrug ABC exporter from *Lactococcus lactis*, when its NBDs were absent (Venter *et al.*, 2003).

References

Alvarez, F.J., Orelle, C., and Davidson A.L. (2010) Functional reconstitution of an ABC transporter in nanodiscs for use in electron paramagnetic resonance spectroscopy. *J Am Chem Soc*. June 25. [Epub ahead of print].

Austermuhle, M.I., Hall, J.A., Klug, C.S., and Davidson, A.L. (2004) Maltose-binding protein is open in the catalytic transition state for ATP hydrolysis during maltose transport. *J Biol Chem* **279**: 28243-28250.

Bahar, I., Lezon, T.R., Bakan, A., and Shrivastava, I.H. (2010) Normal mode analysis of biomolecular structures: functional mechanisms of membrane proteins. *Chem Rev* **110**: 1463-1497.

Berntsson, R.P., Smits, S.H., Schmitt, L., Slotboom, D.J., and Poolman, B. (2010) A structural classification of substrate-binding proteins. *FEBS Lett* **584**:2606-2617.

Biemans-Oldehinkel, E., Doeven, M., and Poolman, B. (2006) ABC transporter architecture and regulatory roles of accessory domains. *FEBS Lett* **580**: 1023-1035.

Blüschke, B., Volkmer-Engert, R., and Schneider, E. (2006) Topography of the surface of the signal transducing protein $EIIA^{Glc}$ that interacts with the MalK subunits of the maltose ATP-binding cassette transporter ($MalFGK_2$) of *Salmonella typhimurium*. *J Biol Chem* **281:** 12833-12840.

Böhm, A., Diez, J., Diederichs, K., Welte, W., and Boos, W. (2002) Structural model of MalK, the ABC subunit of the maltose transporter of *Escherichia coli*: implications for mal gene regulation, inducer exclusion and subunit assembly. *J Biol Chem* **277**: 3708-3717.

Boos, W. and Böhm, A. (2000) Learning new tricks from an old dog: MalT of the *Escherichia coli* maltose system is part of a complex regulatory network. *Trends Genet* **16**: 404-409.

526 Boos, W. and Shuman, H. (1998) Maltose/maltodextrin system of *Escherichia coli*: transport,
527 metabolism and regulation. *Microbiol Mol Biol Rev* **62**: 204-229.
528 Chen J., Lu G., Lin J., Davidson A.L., and Quiocho F.A. (2003) A tweezers-like motion of
529 the ATP-binding cassette dimer in an ABC transport cycle. *Mol Cell* **12:** 651-61.
530 Chen, J., Sharma, S., Quiocho, F.A., and Davidson, A.L. (2001). Trapping the transition state
531 of an ATP-binding cassette transporter: evidence for a concerted mechanism of maltose
532 transport. *Proc Natl Acad Sci USA* **98**: 1525-1530.
533 Covitz, K.-M.Y., Panagiotidis, C.H., Hor, L.-I., Reyes, M., Treptow, N.A. and Shuman, H.A.
534 (1994) Mutations that alter the transmembrane signalling pathway in an ATP binding
535 cassette (ABC) transporter. *EMBO J* **13**: 1752-1759.
536 Danot, O. (2010) The inducer maltotriose binds in the central cavity of the tetratricopeptide-
537 like sensor domain of MalT, a bacterial STAND transcription factor. *Mol Microbiol* **77**:
538 628-641.
539 Dassa, E. and Hofnung, M. (1985) Sequence of gene *malG* in *E. coli* K12: homologies
540 between integral membrane components from binding protein-dependent transport
541 systems. *EMBO J* **4**: 2287–2293.
542 Daus, M.L., Berendt, S., Wuttge, S., and Schneider, E. (2007a) Maltose binding protein
543 (MalE) interacts with periplasmic loops P2 and P1, respectively, of the MalFG subunits of
544 the maltose ATP-binding cassette transporter ($MalFGK_2$) from *Escherichia coli / Salmonella* during the transport cycle. *Mol Microbiol* **66:** 1107-1122.
546 Daus, M.L. Grote, M., and Schneider, E. (2009) The MalF-P2 loop of the ATP-binding
547 cassette (ABC) transporter $MalFGK_2$ from *Escherichia coli / Salmonella enterica* serovar
548 Typhimurium interacts with maltose binding protein (MalE) throughout the catalytic cycle.
549 *J Bacteriol* **191**, 754-761.

Daus, M. L., Grote, M., Müller, P., Doebber, M., Herrmann, A., Steinhoff, H.-J. Dassa, E., and Schneider, E. (2007b) ATP-driven MalK dimer closure and re-opening and conformational changes of the 'EAA' motifs are crucial for function of the maltose ATP-binding cassette transporter ($MalFGK_2$). *J Biol Chem* **282**: 22387-22369.

Daus, M.L., Landmesser, H., Schlosser, A., Müller, P., Herrmann, A., and Schneider, E. (2006) ATP induces conformational changes of periplasmic loop regions of the maltose ATP-binding cassette transporter. *J Biol Chem* **281**: 3856-3865.

Davidson, A.L., Shuman, H.A., and Nikaido, H. (1992). Mechanism of maltose transport in *Escherichia coli*: transmembrane signaling by periplasmic binding proteins. *Proc Natl Acad Sci USA* **89**: 2360-2364.

Davidson, A.L., Dassa, E., Orelle, C., and Chen, J. (2008) Structure, function, and evolution of bacterial ATP-binding cassette systems. *Microbiol Mol Biol Rev* **72**: 317-364.

Dawson, R.J., Hollenstein, K., and Locher, K.P. (2007) Uptake or extrusion: crystal structures of full ABC transporters suggest a common mechanism. *Mol Microbiol.* **65**:250-257.

Deutscher, J., Francke, C., and Postma, P.W. (2006) How phosphotransferase system-related protein phosphorylation regulates carbohydrate metabolism in bacteria. *Microbiol Mol Biol Rev* **70**: 939–1031.

Diederichs, K., Diez, J., Greller, G., Müller, C., Breed, J., Schnell, C., Vonrhein, C., Boos, W., and Welte, W. (2000). Crystal structure of MalK, the ATPase subunit of the trehalose/maltose ABC transporter of the archaeon *Thermococcus litoralis*, *EMBO-J* **19**: 5951-5961.

Doeven, M.K., van den Bogaart, G., Krasnikov, V., and Poolman, B. (2008) Probing receptor-translocator interactions in the oligopeptide ABC transporter by fluorescence correlation spectroscopy. *Biophys J* **94**: 3956-3965.

574 Ehrle, R., Pick, C., Ulrich, R., Hofmann, E., and Ehrmann, M. (1996) Characterization of
575 transmembrane domains 6, 7, and 8 of MalF by mutational analysis. *J Bacteriol* **178**:
576 2255–2262.
577 Ehrmann M., Ehrle R., Hofmann E., Boos W. and Schlösser A. (1998) The ABC maltose
578 transporter. *Mol Microbiol* **29**: 685-694.
579 Eitinger T., Rodionov, D.A., Grote, M., and Schneider, E. (2010) Canonical and ECF-type
580 ATP-binding cassette importers in prokaryotes: diversity in modular organization and
581 cellular functions. *FEMS Microbiol Rev* Apr 23. [Epub ahead of print]
582 Evenäs, J., Tugarinov, V., Skrynnikov, N.R., Goto, N.K., Muhandiram, R., Kay, L.E. (2001)
583 Ligand-induced structural changes to maltodextrin-binding protein as studied by solution
584 NMR spectroscopy. *J Mol Biol* **309**:961-74.
585 Fetsch, E.E., and Davidson, A.L. (2002) Vanadate-catalyzed photocleavage of the signature
586 motif of an ATP-binding cassette (ABC) transporter. *Proc Natl Acad Sci USA* **99**: 9685–
587 9690.
588 Gerber, S., Comellas-Bigler, M., Goetz, B. A., and Locher, K. P. (2008) Structural basis of
589 trans-inhibition in a molybdate/tungstate ABC transporter. *Science* **321**: 246–250.
590 Goetz B.A., Perozo E., and Locher K.P. (2009) Distinct gate conformations of the ABC
591 transporter BtuCD revealed by electron spin resonance spectroscopy and chemical cross-
592 linking. *FEBS Lett* **583**: 266-270.
593 Gould, A.D., Telmer, P.G., and Shilton, B.H. (2009) Stimulation of the maltose transporter
594 ATPase by unliganded maltose binding protein. *Biochemistry* **48**: 8051-8061.
595 Gould, A.D. and Shilton, B.H. (2010) Studies of the maltose transport system reveal a
596 mechanism for coupling ATP hydrolysis to substrate translocation without direct
597 recognition of substrate. *J Biol Chem* **285**: 11290–11296

598 Grote, M., Bordignon, E., Polyhach, Y., Jeschke, G., Steinhoff, H.-J., and Schneider, E.
599 (2008) A comparative EPR study of the nucleotide-binding domains' catalytic cycle in the
600 assembled maltose ABC-importer. *Biophys J* **95**: 2924-2938.
601 Grote, M., Polyhach, Y., Jeschke, G., Steinhoff, H.-J., Schneider, E., and Bordignon, E.
602 (2009) Transmembrane signaling in the maltose ABC transporter $MalFGK_2$-E. Periplasmic
603 MalF-P2 loop communicates substrate availability to the ATP-bound MalK dimer. *J Biol*
604 *Chem* **284**: 17521-17526.
605 Hebbeln, P., Rodionov, D.A., Alfandega, A., and Eitinger, T. (2007) Biotin uptake in
606 prokaryotes by solute transporters with an optional ATP-binding cassette-containing
607 module. *Proc Natl Acad Sci USA* **104**: 2909-2914.
608 Holland, I.B., Cole, S.P.C., Kuchler, K., and Higgins, C.F. (eds.) (2003) ABC proteins: From
609 bacteria to man. Elsevier, Amsterdam.
610 Hollenstein, K., Frei, D.C., and Locher, K.P. (2007) Structure of an ABC transporter in
611 complex with its binding protein. *Nature* **446**:213-216.
612 Hopfner, K.-P., Karcher, A., Shin, D.S., Craig, L., Arthur, L.M., Carney, J.P., and Tainer, J.A.
613 (2000). Structural biology of Rad50 ATPase: ATP-driven conformational control in DNA
614 double-strand break repair and the ABC-ATPase superfamily. *Cell* **101**: 789-800.
615 Hunke, S., Mourez, M., Jéhanno, M., Dassa, E., and Schneider, E. (2000) ATP modulates
616 subunit-subunit interactions in an ATP-binding cassette transporter ($MalFGK_2$) determined
617 by site-directed chemical cross-linking. *J Biol Chem* **275**: 15526-15534.
618 Hvorup, R.N., Goetz, B.A., Niederer, M., Hollenstein, K., Perozo, E., and Locher, K.P.
619 (2007) Asymmetry in the structure of the ABC transporter-binding protein complex
620 BtuCD-BtuF. *Science* **317**: 1387-1390.
621 Jacso, T., Grote, M., Daus, M.L., Schmieder, P., Keller, S., Schneider, E., and Reif, B. (2009)
622 The periplasmic loop P2 of the MalF subunit of the maltose ATP binding cassette

transporter is sufficient to bind the maltose binding protein MalE. *Biochemistry* **48**: 2216-2225.

Joly, N., Böhm, A., Boos, W., and Richet, E. (2004) MalK, the ATP-binding cassette component of the *Escherichia coli* maltodextrin transporter, inhibits the transcriptional activator MalT by antagonizing inducer binding. *J Biol Chem* **279**: 33123-33130.

Jones, P.M., O'Mara, M.L., and George, A.M. (2009) ABC transporters: a riddle wrapped in a mystery inside an enigma. *Trends Biochem. Sci* **34**: 520-531

Kadaba, N. S., Kaiser, J. T., Johnson, E., Lee, A., and Rees D. C. (2008) The high-affinity *E. coli* methionine ABC transporter: structure and allosteric regulation. *Science* **321**:250-253.

Khare, D., Oldham, M., Orelle, C., Davidson. A.L., and Chen, J. (2009) Alternating access in maltose transporter mediated by rigid-body rotations. *Mol Cell* **33**: 528-536.

Landmesser, H., Stein, A., Blüschke, B., Brinkmann, M., Hunke, S., and Schneider, E. (2002) Large-scale purification, dissociation and functional reassembly of the maltose ATP-binding cassette transporter ($MalFGK_2$) of *Salmonella typhimurium. Biochim Biophys Acta* **1565**: 64-72.

Larquet, E., Schreiber, V., Boisset, N., and Richet, E. (2004) Oligomeric assemblies of the *Escherichia coli* MalT transcriptional activator revealed by cryo-electron microscopy and image processing. *J Mol Biol* **343**: 1159-1169.

Leipe, D.D., Koonin, E.V., and Aravind, L. (2004) STAND, a class of P-loop NTPases including animal and plant regulators of programmed cell death: multiple, complex domain architectures, unusual phyletic patterns, and evolution by horizontal gene transfer. *J Mol Biol* **343**: 1-28.

Lewinson, O., Lee, A.T., Locher, K.P., and Rees, D.C. (2010) A distinct mechanism for the ABC transporter BtuCD–BtuF revealed by the dynamics of complex formation. *Nature Struct Mol Biol* **17**: 332–338.

Locher, K (2009) Structure and mechanism of ATP-binding cassette transporters. *Phil Trans R Soc B* **364:** 239-245.

Locher, K.P., Lee, A.T., and Rees, D.C. (2002) The *E. coli* BtuCD structure: a framework for ABC transporter architecture and mechanism. *Science* **296**:1091-1098.

Lu, G., Westbrooks, J. M., Davidson, A. L., and Chen, J. (2005) ATP hydrolysis is required to reset the ATP-binding cassette dimer into the resting-state conformation. *Proc Natl Acad Sci USA* **102**: 17969-17974.

Mannering, D.E., Sharma, S., and Davidson, A.L. (2001) Demonstration of conformational changes associated with activation of the maltose transport complex. *J Biol Chem* **276**:12362-12388.

Marquenet, E. and Richet, E. (2007) How integration of positive and negative regulatory signals by a STAND signaling protein depends on ATP hydrolysis. *Mol Cell* **28**: 187-199.

Morbach, S., Tebbe, S., and Schneider, E. (1993) The ABC transporter for maltose/maltodextrins of *Salmonella typhimurium*: Biochemical characterization of the ATPase activity associated with the purified MalK subunit. *J Biol Chem* **268**: 18617-18621.

Mourez, M., Hofnung, M., and Dassa, E. (1997) Subunit interactions in ABC transporters: a conserved sequence in hydrophobic membrane proteins of periplasmic permeases defines an important site of interaction with the ATPase subunits. *EMBO J* **16**:3066-3077.

Oldham, M. L., Khare, D., Quiocho, F.A., Davidson, A.L., and Chen, J. (2007). Crystal structure of a catalytic intermediate of the maltose transporter. *Nature* **450**: 515-522.

Oloo, E.O., Fung, E.Y., and Tieleman, D.P. (2006) The dynamics of the MgATP-driven closure of MalK, the energy-transducing subunit of the maltose ABC transporter. *J Biol Chem* **281**: 28397-28407.

672 Orelle C., Ayvaz T., Everly R.M., Klug C.S., and Davidson A.L. (2008) Both maltose-
673 binding protein and ATP are required for nucleotide-binding domain closure in the intact
674 maltose ABC transporter. *Proc Natl Acad Sci USA* **105**: 12837-12842.
675 Oswald, C., Holland, I.B., and Schmitt, L. (2006) The motor domains of ABC-transporters.
676 What can structures tell us? *Naunyn-Schmiedeberg's Arch Pharmacol* **372**: 385–399.
677 Pinkett, H.W., Lee, A.T., Lum, P., Locher, K.P., and Rees, D.C. (2007) An inward-facing
678 conformation of a putative metal-chelate-type ABC transporter. *Science* **315**:373-377.
679 Quiocho, F.A. and Ledvina, P.S. (1996) Atomic structure and specificity of bacterial
680 periplasmic receptors for active transport and chemotaxis: variation of common themes.
681 *Mol Microbiol* **20**: 17-25.
682 Ranquin, A., and van Gelder, P. (2004) Maltoporin: sugar for physics and biology. *Res*
683 *Microbiol* **155**: 611-616.
684 Richet, E., Joly, N., and Danot, O. (2005) Two domains of MalT, the activator of the
685 *Escherichia coli* maltose regulon, bear determinants essential for anti-activation by MalK.
686 *J Mol Biol* **347**: 1-10.
687 Rodionov, D.A., Hebbeln, P., Gelfand, M.S., and Eitinger, T. (2006) Comparative and
688 functional genomic analysis of prokaryotic nickel and cobalt uptake transporters: evidence
689 for a novel group of ATP-binding cassette transporters. *J Bacteriol* **188**: 317-327.
690 Rodionov, D. A., Hebbeln, P., Eudes, A., ter Beek, J., Rodionova, I. A., Erkens, G. B.,
691 Slotboom, D. J., Gelfand, M. S., Osterman, A. L., Hanson, A. D., and Eitinger, T. (2009) A
692 novel class of modular transporters for vitamins in prokaryotes. *J Bacteriol* **191**:42-51.
693 Samanta, S., Ayvaz, T., Reyes, M., Shuman, H.A., Chen, J., and Davidson, A.L. (2003)
694 Disulfide cross-linking reveals a site of stable interaction between C-terminal regulatory
695 domains of the two MalK subunits in the maltose transport complex. *J Biol Chem*
696 **278**:35265–35271.

Sharff, A.J., Rodseth, L.E., Spurlino, J.C. and Quiocho, F.A. (1992) Crystallographic evidence of a large ligand-induced hinge-twist motion between the two domains of the maltodextrin binding protein involved in active transport and chemotaxis. *Biochemistry* **31**: 10657-10663.

Shilton, B.H. (2008) The dynamics of the MBP-MalFGK(2) interaction: a prototype for binding protein dependent ABC-transporter systems. *Biochim Biophys Acta* **1778**: 1772-1780.

Shilton, B.H., Flocco, M.M., Nilsson, M., and Mowbray, S.L. (1996) Conformational changes of three periplasmic receptors for bacterial chemotaxis and transport: the maltose-, glucose/galactose- and ribose-binding proteins. *J Mol Biol* **264**:350-63.

Spurlino, J.C., Lu, G.-Y. and Quiocho, F.A. (1991) The 2.3-Å resolution structure of the maltose- or maltodextrin-binding protein, a primary receptor of bacterial active transport and chemotaxis. *J Biol Chem* **266**: 5202-5219.

Steegborn, C., Danot, O., Huber, R., and Clausen, T. (2001) Crystal structure of transcription factor MalT domain III: a domain helix repeat fold implicated in regulated oligomerization. *Structure* **9**: 1051-1060.

Steinke, A., Grau, S., Davidson, A., Hofmann, E., and Ehrmann, M. (2001) Characterization of transmembrane segments 3, 4, and 5 of MalF by mutational analysis. *J Bacteriol* **183**: 375–381.

Stockner T., Vogel H. J. and Tieleman, D. P. (2005) A salt-bridge motif involved in ligand binding and large-scale domain motions of the maltose-binding protein. *Biophys J* **89**: 3362-3371

Tang C., Schwieters C.D. and Clore G.M. (2007) Open-to-close transition in apo maltose-binding protein observed by paramagnetic NMR. *Nature* **449**: 1078-1082.

721 Tapia, M.I., Mourez, M., Hofnung, M., and Dassa, E. (1999) Structure-function study of
722 MalF protein by random mutagenesis. *J Bacteriol* **181:** 2267–2272.
723 Venter, H., Shilling, R.A., Velamakanni, S., Balakrishnan, L., and van Veen, H.W. (2003) An
724 ABC transporter with a secondary-active multidrug translocator domain. *Nature* **426**: 866-
725 870.
726 Wang, G., Peterkofsky, A., and Clore, G.M. (2000) A novel membrane anchor function for
727 the N-terminal amphipathic sequence of the signal-transducing protein IIA^{Glucose} of the
728 *Escherichia coli* phosphotransferase system. *J Biol Chem.* **275**:39811-39814.
729 Wen, P.-C., and Tajkhorshid, E. (2008) Dimer opening of the nucleotide binding domains of
730 ABC transporters after ATP hydrolysis. *Biophys J* **95**: 5100-5110.
731 Zhang, Y., Gardina, P.J., Kuebler, A.S., Kang, H.S., Christopher, J.A., and Manson, M.D.
732 (1999) Model of maltose-binding protein/chemoreceptor complex supports intrasubunit
733 signaling mechanism. *Proc Nat Acad Sci USA* **96**: 939-944.
734 Zou, P., and Mchaourab, H.S. (2010) Increased sensitivity and extended range of distance
735 measurements in spin-labeled membrane proteins: Q-band double electron-electron
736 resonance and nanoscale bilayers. *Biophys J* **98**: L18–L20.
737

738 **Acknowledgements**

739 Work from the authors' laboratories was supported by the Deutsche Forschungsmeinschaft
740 (SCHN 274/9-3; SFB 449, TP B14; to E.S.)

741

742

743

Figure legends

Fig. 1. Components of the maltose transport system. Maltose (grey, space-fill representation) and maltodextrins (not shown) cross the outer membrane (OM) via passage through homotrimeric maltoporin (in *E. coli* also known as LamB due to its function as receptor for bacteriophage lambda). In the periplasm, maltose is bound by maltose binding protein, MalE or MBP, thereby shifting the protein from the open to the closed conformation. Translocation of the substrate across the inner (cytoplasmic) membrane (IM) is initiated by interaction of liganded MalE with periplasmic loop regions of the transport complex composed of the pore-forming subunits MalF (blue) and MalG (magenta) and a homodimer of the ATP-binding subunit, MalK (in red and green). The figure was drawn using the pdb codes 1MPM (maltoporin with bound maltose), 1JW4 (unliganded MalE), 1ANF (MalE with bound maltose), 3FH6 (transport complex, apo-state), and 2R6G (transport complex, catalytic intermediate). Please note that for simplicity the asymmetric nature of the outer membrane (the inner and outer leaflet being constituted by phospholipids and lipopolysaccharides, respectively) is not depicted. Structures not necessarily drawn to scale.

Fig. 2. Dynamics of the MalK dimer. Stereo view of three known crystal structures (side and top views) of the MalK dimer (Chen *et al.*, 2003; Lu *et al.*, 2005) superimposed on the C-terminal regulatory domains. The overlay demonstrates the conformational changes of the N-terminal (dynamic) domains from the open apo-state (red) to the closed ATP-bound state (light green) and the reopening after ATP hydrolysis (ADP-bound, semi-open state, green). The C-terminal (rigid) domains do not undergo significant motions. The PDB codes of the structures presented are depicted in the figure.

Fig. 3. Current dynamic model for ATP-dependent maltose uptake in $MalFGK_2$ based on the data discussed in the review. The equilibrium between an open apo-, a closed apo- and a

768 closed holo-form of MalE is presented, with the first two species shown to bind to $MalFGK_2$
769 to induce a futile ATP hydrolysis cycle (within grey squared brackets, right hand side of the
770 figure). The TMDs are shown to interchange between a cytoplasmic-open (ADP-bound) and a
771 periplasmic-open (ATP-bound) state (alternating mechanism). The correspondence of three
772 different states for $MalK_2$ and MalF-P2 is indicated by the same colour coding, the flexibility
773 of MalF-P2 in the absence of MalE is indicated by a dotted green ellipse. Transitions between
774 the two conformers highlighted in the red box represent ATP-dependent import of maltose in
775 the cell, with the stars denoting the instable nature of the ATP-bound intermediate. The dotted
776 box highlights a short-lived intermediate (the apo state) in the cell. The uncoupled state of an
777 ATP-bound transporter in detergent solution is indicated within black squared brackets. X-ray
778 snapshots are superimposed to the models where available. (Modified from Fig. 5 in Grote *et*
779 *al.*, 2009).

780 **Fig. 4.** Model of interaction between the MalK dimer and $EIIA^{Glc}$. The model was created by
781 the Zdock server at http://zdock.bu.edu/ using pdb codes 2AWO (MalK dimer complexed
782 with ADP) and 1F3G ($EIIA^{Glc}$). *Left panel*: residues of $MalK_2$ selected for modelling that are
783 known to cause resistance to $EIIA^{Glc}$ when mutated (E119, A124, R228, F241, S282: Samanta
784 *et al.,* 2003 and further references therein; R324: Wuttge, Kuhnert, Schneider, unpublished
785 observation). Other residues considered by Samanta *et al.* (2003) were omitted as they lie
786 somewhat offside the proposed binding surface (G278, G302) or are not surface exposed
787 (G284). Including these residues did not result in the prediction of a model. Thus, their impact
788 on $EIIA^{Glc}$ binding might rather be indirect. Including S322 (Samanta *et al.*, 2003) resulted in
789 the same model. MalK chains A (red) and B (green) are shown in space-fill representation.
790 *Right panel*: Zdock result showing $EIIA^{Glc}$ (grey) with selected residues (cyan) that when
791 mutated abolish the inhibitory activity (Blüschke *et al.*, 2006) or form cross-links with MalK

(Wuttge, Kuhnert, Schneider, unpublished observation). Please note that the program does not predict the stoichiometry between interacting proteins.

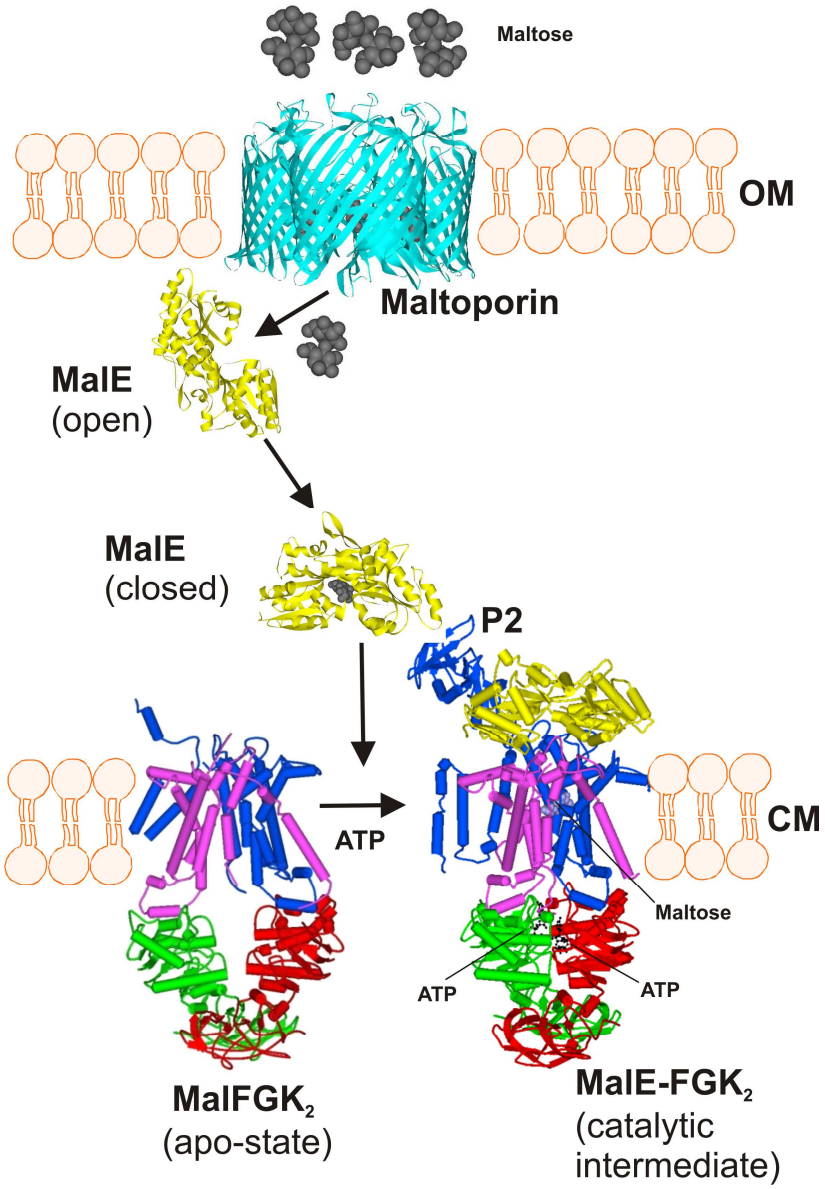

195x288mm (300 x 300 DPI)

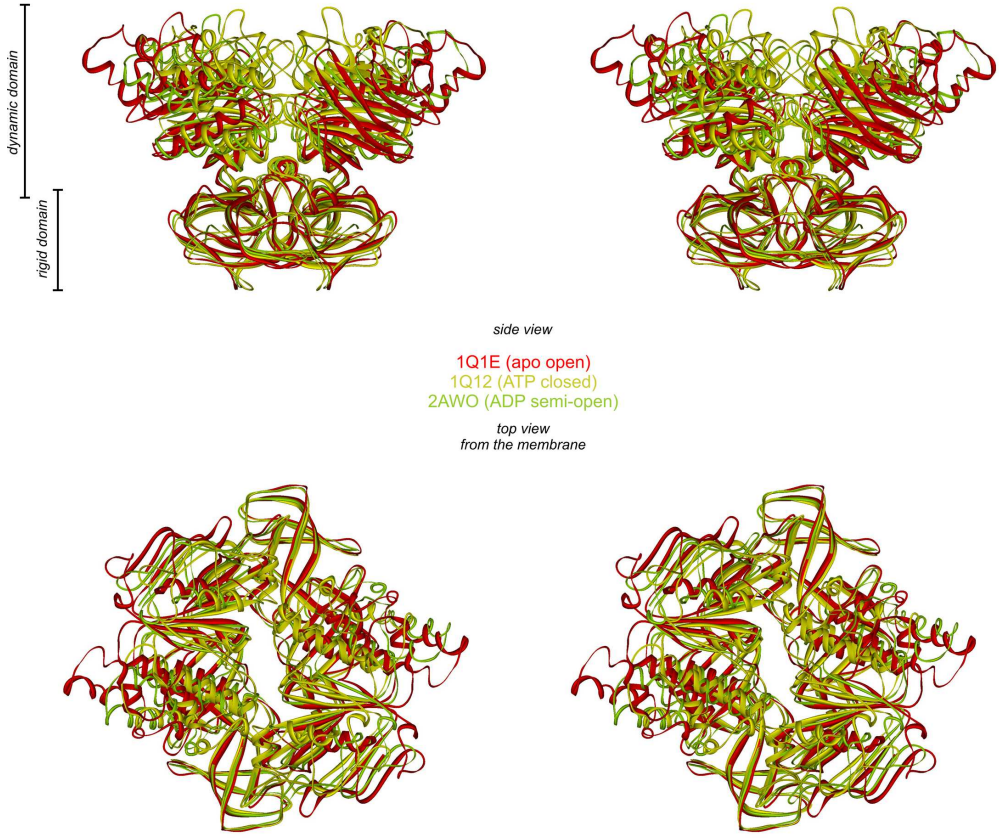

184x165mm (300 x 300 DPI)

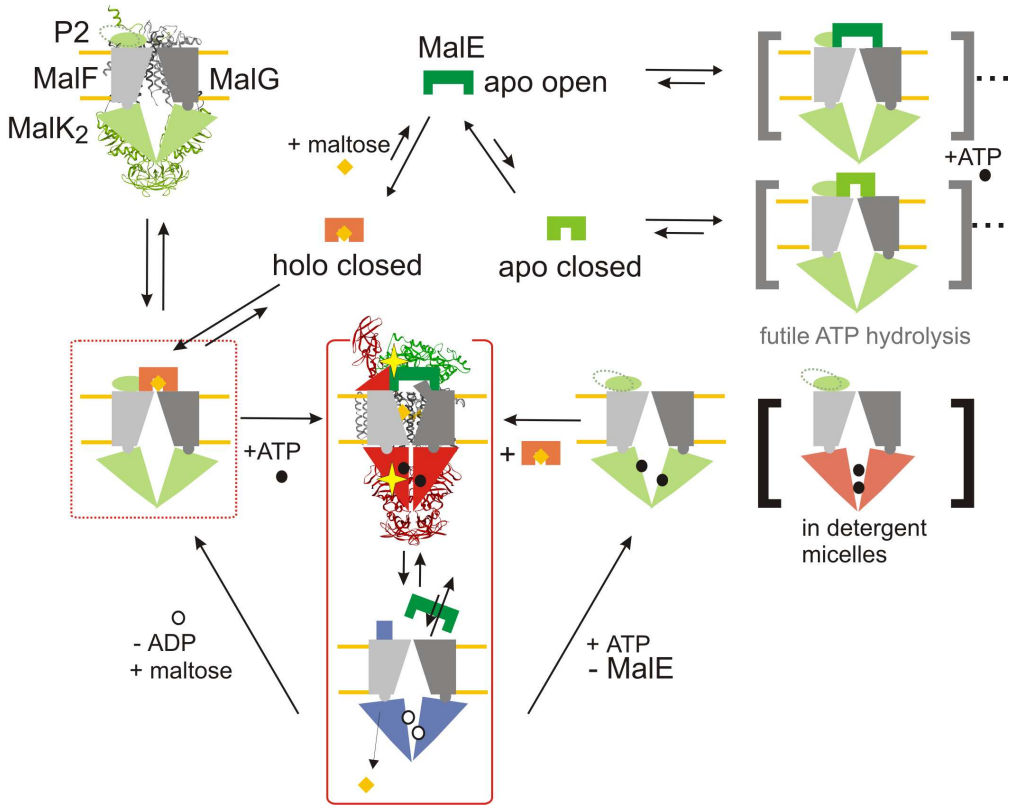

178x143mm (300 x 300 DPI)

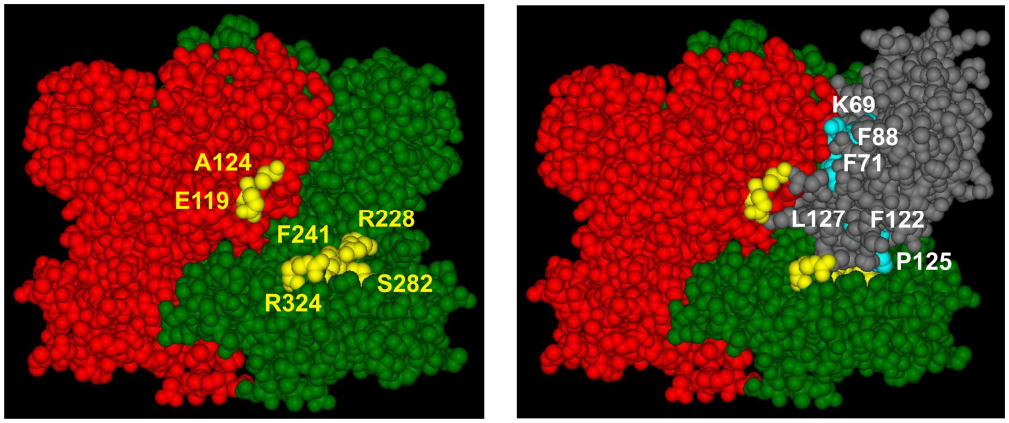

262x109mm (300 x 300 DPI)